Cerebral Cortex, November 2018;28: 4049–4062

doi: 10.1093/cercor/bhy198
Advance Access Publication Date: 31 August 2018
Original Article

ORIGINAL ARTICLE

KCC2 Regulates Dendritic Spine Formation in a Brain-Region Specific and BDNF Dependent Manner

Patricia Nora Awad[1,2], Clara Akofa Amegandjin[1,2], Joanna Szczurkowska[3], Josianne Nuñes Carriço[2], Antônia Samia Fernandes do Nascimento[2], Elie Baho[1,2], Bidisha Chattopadhyaya[1,2], Laura Cancedda[3,4], Lionel Carmant[1,2] and Graziella Di Cristo[1,2]

[1]Department of Neurosciences, Université de Montréal, Montréal, Québec, Canada H3C 3J7, [2]CHU Sainte-Justine Research Center, Montréal, Québec, Canada H3T 1C5, [3]Neuroscience and Brain Technologies, Instituto Italiano di Tecnologia, Genova 16163, Italy and [4]Telethon Dulbecco Institute, Italy

Address correspondence to Graziella Di Cristo, Research Center, CHU Sainte-Justine/Université de Montréal, Neuroscience Department, 3175 Côte-Sainte-Catherine, Montréal, Québec, Canada H3T 1C5. Email: graziella.dicristo@recherche-ste-justine.qc.ca

Abstract

KCC2 is the major chloride extruder in neurons. The spatiotemporal regulation of KCC2 expression orchestrates the developmental shift towards inhibitory GABAergic drive and the formation of glutamatergic synapses. Whether KCC2's role in synapse formation is similar in different brain regions is unknown. First, we found that KCC2 subcellular localization, but not overall KCC2 expression levels, differed between cortex and hippocampus during the first postnatal week. We performed site-specific in utero electroporation of KCC2 cDNA to target either hippocampal CA1 or somatosensory cortical pyramidal neurons. We found that a premature expression of KCC2 significantly decreased spine density in CA1 neurons, while it had the opposite effect in cortical neurons. These effects were cell autonomous, because single-cell biolistic overexpression of KCC2 in hippocampal and cortical organotypic cultures also induced a reduction and an increase of dendritic spine density, respectively. In addition, we found that the effects of its premature expression on spine density were dependent on BDNF levels. Finally, we showed that the effects of KCC2 on dendritic spine were dependent on its chloride transporter function in the hippocampus, contrary to what was observed in cortex. Altogether, these results demonstrate that KCC2 regulation of dendritic spine development, and its underlying mechanisms, are brain-region specific.

Key words: brain-derived neurotrophic factor, dendritic spines, development, KCC2, synapse formation

Introduction

Proper function of neural circuits requires the orchestrated formation of trillions of synapses. During the last decades, much effort has been directed towards understanding how synapses form, a necessary step to better comprehend how the brain is built during normal development and how this process goes awry in diseases characterized by altered synapse function. The vast majority of studies have often focused on specific neuron cell types from specific brain regions. However, one important question is whether molecular mechanisms

regulating synapse formation in a specific neuronal cell type (e.g., glutamatergic neurons) can be generalized to similar neurons localized in different brain regions (e.g., in the cortex vs. the hippocampus).

KCC2 is a potassium-chloride cotransporter, the only member of the Cation Chloride Cotransporter family that is almost exclusively expressed in neurons (Kaila, Price, et al. 2014). The increase in KCC2 expression during development is responsible for the shift of GABAergic drive towards more inhibitory activity, by decreasing intracellular [Cl^-] (Ben-Ari et al. 1989; Chudotvorova et al. 2005; Fiumelli et al. 2005; Lee et al. 2005). In addition, it has been suggested that KCC2 can modulate glutamatergic synapse development and function, via ion-transport independent mechanisms (Li et al. 2007; Gauvain et al. 2011; Fiumelli et al. 2013; Chevy et al. 2015). For example, removing KCC2 in immature cortical neurons prevented spine maturation altogether, leading to an increase of filopodia protrusions (Li et al. 2007). Conversely, removing KCC2 in mature hippocampal neurons, after spine formation and when KCC2 expression reached its plateau, did not affect spine density but reduced the efficacy of excitatory synapses, through an alteration of AMPA receptor aggregation (Gauvain et al. 2011; Chevy et al. 2015). Interestingly, these effects were not due to reduction of transporter activity, but to altered interactions of KCC2 with the cytoskeleton (Li et al. 2007; Gauvain et al. 2011). Consistent with these findings, premature expression of KCC2 induced by in utero electroporation of its cDNA in cortical pyramidal cells caused a long-lasting increase in dendritic spine density through a mechanism that was independent of its ion transporter function (Fiumelli et al. 2013). All together, these studies suggest that KCC2 expression levels control dendritic spine density and AMPA receptor aggregation in pyramidal cells, by modulating cytoskeleton dynamics. However, seemingly in contrast with this hypothesis, embryonic (E18.5) $KCC2^{-/-}$ hippocampi showed increased GABAergic and glutamatergic synapse density and a higher frequency of spontaneous glutamatergic and GABAergic postsynaptic currents than wild-type age-matched neurons (Khalilov et al. 2011). One possible explanation for this discrepancy is that the effects of KCC2 alterations on spine formation are brain-region dependent, at least during early developmental stages. KCC2 has gained a lot of attention recently because alterations of its function and expression levels have been reported in several neurodevelopmental disorders, including epilepsy and autism, both in humans and rodent models (Ferrini and De Koninck 2013; Kaila, Ruusuvuori, et al. 2014; Merner et al. 2015; Awad et al. 2016; Tang et al. 2016; Di Cristo et al. 2018). Therefore, elucidating the precise role, and underlying mechanisms of KCC2 on synapse formation in different brain region is a first, critical step to understand how alterations of its expression or function may contribute to specific circuit and cognitive deficits.

Here, we report that KCC2 subcellular localization in pyramidal neurons during the first postnatal week was significantly different in the CA1 region of the hippocampus and the somatosensory cortex. We further found that premature expression of KCC2 by targeted in utero electroporation caused opposite effects on spine density in the 2 regions and that KCC2-induced spine loss in the hippocampus was dependent on its transporter activity. Finally, we showed that increasing the levels of Brain Derived Neurotrophic Factor (BDNF), a potent regulator of KCC2 expression and activity in the immature brain (Ludwig et al. 2011; Puskarjov et al. 2015), was sufficient to block the spine density increase induced by KCC2 premature expression in cortical pyramidal neurons.

Materials and Methods

Animals

Sprague–Dawley pups were obtained from Charles River Laboratories (St. Constant, Quebec, Canada) at postnatal day 1 (P1) or pregnant at gestational day 10 (E10). Pups were culled to 12 per dam, matched by gender, weighed and kept with their mother in a 12 h light/dark cycle with food and water ad libitum. Animal care and use conformed to institutional policies and guidelines (CIBPAR, Sainte-Justine Hospital Research Centre, Université de Montréal, Montreal, Quebec, Canada).

Western Blot

Whole lysate proteins were extracted from hippocampal and somatosensory cortex tissue in vivo or hippocampal and cortical organotypic cultures, at different ages in vivo or days in vitro, as indicated in the legends, following the previously described protocol (Ouardouz et al. 2010). To obtain membrane protein fractions, samples were homogenized in 5 vol of HB (300 mM sucrose/10 mM Tris–HCl, pH 7.5/1 mM EDTA/protease inhibitor mixture) and centrifuged at 1000 × *g* for 10 min at 4 °C. The pellet was washed in 0.5 vol HB and used as the nuclear fraction. The supernatants was centrifuged at 17 000 × *g* for 15 min at 4 °C, yielding the mitochondria fraction. The supernatant was further separated by ultracentrifugation at 100 000 × *g* for 1 h. The pellet and supernatant were used as the membrane and cytosol fractions, respectively.

For organotypic slice cultures, at least 3–4 slices per animal were pooled in a sample, in order to have enough proteins from whole lysates. Each experimental group included 3–5 animals. Membranes were probed with the following primary antibodies: anti-KCC2 1:1000 (rabbit polyclonal IgG; Cat. no. 07-432, Millipore), 1:200 anti-BDNF (cat#N-20: sc-546, Santa-Cruz Biotechnology, Inc.), anti-glyceraldehyde-3-phosphate dehydrogenase 1:4000 (GAPDH, mouse monoclonal IgG; Cat. no. AM4300; Applied Biosystems) and anti-β dystroglycan 1:3000 (rabbit polyclonal IgG, Cat no. ab43125, Abcam). Specificity of BDNF antibody was verified using tissue from a $BDNF^{-/-}$ mouse and a wild-type littermate (data not shown). All samples were run simultaneously. Bands were quantified using Image J software. The intensity of KCC2 and BDNF bands were normalized over the intensity of the GAPDH band for whole lysates or of the β dystroglycan band for membrane fractions, in the same lane (internal loading control).

Immunolabeling Experiments

Brains were perfused with saline (0.9% NaCl) followed by 4% paraformaldehyde/phosphate buffer, pH 7.4, then cryoprotected in 30% sucrose/PBS, and frozen in Tissue Tek. Brains were sectioned (80 µm thick for in utero electroporation experiment, 40 µm for immunostaining of KCC2) using a cryostat (Leica). Slices were blocked in 10% NGS and 0.3% Triton for 2 h at room temperature, and incubated overnight at 4 °C in 5% NGS, 0.1% Triton and the following primary antibodies—NeuN, 1:400 (mouse monoclonal, Cat. no. MAB377 Millipore); KCC2, 1:200 (rabbit polyclonal, Cat. no. 07-432 Millipore); GFP, 1:500 (chicken polyclonal, Cat. no. Ab13970 Abcam). The following secondary antibodies were used: anti-mouse Alexa 633-conjugated goat IgG and anti-rabbit Alexa 488-conjugated goat IgG (1:400; Molecular Probes, Invitrogen) or Alexa 488 goat anti-chicken IgY H&L (1:500, Cat. no. Ab150169 Abcam). NeuN staining was used to unequivocally identify the CA1 region in hippocampal slices. GFP immunostaining was used to enhance

GFP signal so we could reliably detect thin spines in all imaged cells. For the quantification of KCC2 expression and localization in vivo, we imaged the somatosensory cortex (SSCx) and the CA1 hippocampal region in 3–4 sections/animal. Confocal stacks were acquired using a Leica SP8 confocal microscope and a ×63 (glycerol, NA 1.3) objective and a z step of 0.5μm. The classification of the KCC2-positive neurons to groups with and without signal in the plasmalemma was done manually relying on the detectable fluorescence band on the periphery of the cell. To quantify KCC2 expression levels in the plasmalemmal compartment in organotypic cultures, either naïve or treated with BDNF, pyramidal cell somata were outlined, using NeuN staining as reference, then an outer profile was traced at about 1μm from the inner one and the intensity levels were measured, after background subtraction, using the quantification tools included in Leica LAS X software. 5–6 organotypic cultures were imaged per experimental groups, using a Leica SP8, as described above. All analysis were done blind to the age and treatment.

Organotypic Slice Culture

Slice culture preparation was essentially as described in Chattopadhyaya et al. (2004). Mouse pups at postnatal day 4 (P4) for cortical slices and at P6 for hippocampal slices were decapitated, and brains were rapidly removed and immersed in ice-cold culture medium (containing MEM, 20% horse serum, 1 mM glutamine, 13 mM glucose, 1 mM $CaCl_2$, 2 mM $MgSO_4$, 0.5 μm/mL insulin, 30 mM HEPES, 5 mM $NaHCO_3$, and 0.001% ascorbic acid). Coronal brain slices of hippocampus or cortex, 400 μm thick, were cut with a Chopper (Stoelting, Wood Dale, IL) into ice-cold culture medium. Slices were then placed on transparent Millicell membrane inserts (Millipore, Bedford, MA), usually 3–5 slices/insert, in 30 mm Petri dishes containing 0.75 mL of culture medium. Finally, they were incubated in a humidified incubator at 34 °C with a 5% CO_2-enriched atmosphere, and the medium was changed 3 times per week. All procedures were performed under sterile conditions. Constructs to be transfected were incorporated into "bullets" made using 1.6 μm gold particles coated with 30 μg of each of the plasmids of interest. These bullets were used to biolistically transfect slices by gene gun (Bio-Rad, Hercules, CA) at high pressure (180 Pa). Cultures were biolistically tranfected with either pCI-KCC2wt-IRES-eGFP or pCI-KCC2 C568A-IRES-eGPF together with pCI-tdTomato or pCI-GFP, from equivalent postnatal day (EP) 6 to EP20. We found that the colocalization of GFP and tdTomato signals was 100% when cultures were shot with pCI-KCC2wt-IRES-eGFP or pCI-KCC2 C568A-IRES-eGPF and pCI-tdTomato. Therefore, in parallel experiments, we shot pCI-GFP to maximize detections of thin dendritic spines, as GFP provided the best signal for our confocal system configuration. Transfected slices were incubated under the same conditions as described above, before fixation and imaging. In specific experiments described in the Result Section, we treated cortical cultures with human BDNF (50 ng/mL, Alomone cat#B-250) from the day of culture preparation to EP9 (to analyze the effect of BDNF treatment on KCC2 localization at the plasmalemmal compartment) or until EP20 (for spine analysis). To control for variability due to slice preparation, we prepared one plate from each pup, and treated half of the plate with BDNF and half with vehicle solutions. For immunolabeling of organotypic culture, slices were fixed with 4% PFA, then cryoprotected in 30% sucrose/PBS and frozen/thawed to increase antibody penetration. Slices were then incubated with the appropriate primary and secondary antibodies, and imaged, as describe above.

In Utero Electroporation

In utero electroporation was performed essentially as described in (Awad et al. 2016). The day of mating was defined as embryonic day zero (E0), and the day of birth was defined as postnatal day zero (P0). E17 timed-pregnant Sprague Dawley rats were anesthetized with isoflurane (induction, 4%; surgery, 2%), and the uterine horns were exposed by laparotomy. The DNA (2 μg/μL in distilled water) together with the dye Fast Green (0.3 mg mL^{-1}; Sigma, St Louis, MO, USA) was injected (5 μL) through the uterine wall into one of the lateral ventricles of each embryo by a sterile 30-gauge needle. After soaking the uterine horn with a phosphate-buffered saline (PBS) solution, the embryo's head was carefully held between tweezer-type circular electrodes (10 mm diameter; Nepa Gene, Bulldog Bio, Canada) to transfect the cortex. To target the hippocampus, we used the tweezer-type circular electrodes as well, while a third electrode (7 × 6 × 1 mm^3, platinum-plated copper) was accurately positioned for electroporation (Dal Maschio et al. 2012). For the electroporation, 5 electrical pulses (amplitude, 50 V; duration, 50 ms; intervals, 150 ms) were delivered with a square-wave electroporation generator (CUY21EDIT, Nepa Gene; ECM 830, BTX, Harvard Apparatus). After electroporation, the uterine horns were returned into the abdominal cavity, and embryos allowed continuing their normal development. At P20, rats were fixed by transcardial perfusion with 4% PFA in phosphate buffer (0.1 M, pH 7.4)

The cDNA encoding KCC2 full-length WT (KCC2wt), the loss-of-function mutant KCC2-C568A, and the transporter-dead mutants C-term KCC2 (KCC2-CTD) and delta N-term KCC2 (KCC2-ΔNTD) were previously described and cloned into pCAG-IRES-EGFP (Fiumelli et al. 2013). The pCAG vector bears a modified chicken β-actin promoter with a cytomegalovirus immediate-early enhancer that directs high and persistent expression levels in neurons in vivo (Niwa et al. 1991). The vectors expressing wild-type or mutant KCC2 were cotransfected with pCAG-IRES-tdTomato or pCAG-GFP. Finally, pCAG-IRES-tdTomato or pCAG-GFP plasmids alone were used as a control. These plasmids combination are referred thereafter as "KCC2wt," "KCC2 C568A," "KCC2 CTD," "KCC2 ΔNTD," and "Ctrl," respectively.

Confocal Imaging of Pyramidal Cells and Dendritic Spine Analysis

The 2–3 labeled typical pyramidal neurons were randomly selected from CA1 area or the somatosensory cortex of each analyzed animal or organotypic cultures. Image stacks of basal dendrites were acquired at 0.5 μm intervals using a confocal microscope (Leica SPE or SP8) with a ×63 glycerol objective (×63, NA 1.3), and then analyzed with Neurolucida (MicroBrightField) software. To avoid problems in identifying dendrite provenance in highly transfected areas, we analyzed only the basal dendrites included in 4 identically sized stacks centered around the soma, which in our imaging conditions represent the first 120 μm of basal dendrites originating from the soma. Low magnification (×10 or ×20) images of each analyzed pyramidal cell were acquired as reference of cell localization and overall morphology.

Spine density, spine morphology and spine length were analyzed and quantified in 3D using Neurolucida software (MicroBrightField), as described in Awad et al. (2016). We classified

spines as mushroom spines, identified by a clearly distinguishable enlargement of the head of the spine (compared with the neck); stubby spines, identified as structures with equal thickness between head and neck (minimum 0.3 µm thick); thin spines as long and thin protrusions lacking a clearly defined head (maximum of 0.3 µm thick). Values for animals belonging to the same experimental group were not statistically different and were pooled. All quantification was done blind to the treatment.

Statistical Analysis

Differences between 2 experimental groups were assessed using unpaired *t*-test for normally distributed data and Mann–Whitney test for not normally distributed data, except for the experiment investigating KCC2 levels in the membrane fraction of cortical organotypic cultures treated with vehicle or BDNF, which was analyzed by paired *t*-test (organotypic cultures prepared from a single mouse were treated half with vehicle and half with BDNF). Differences between 3 or more experimental groups were assessed with one-way ANOVA and Tukey's multiple comparisons test. For non-normally distributed data, non-parametric Kruskal–Wallis one-way ANOVA test was used. Two-way ANOVA with Holm–Sidak's multiple comparison post hoc analysis was used to determine the relative contribution of age (factor 1) and brain region (factor 2) on KCC2 expression levels. Cumulative distributions of spine length or spine diameter were plotted as follow: for each cell, spine length or spine diameter values were ordered by cumulative distribution; then values were binned. For all cells belonging to the same experimental group, the mean ± standard error of mean (SEM) of each bin was calculated and plotted. Statistical differences of cumulative distribution were analyzed using the Kolmogorov–Smirnov (KS) test. All results are expressed as mean ± SEM. Spine density, length and diameter analysis were represented with Tukey boxplots (median ± 1.5 × interquartile range, IQR; box represents first-third quartile). Statistical analysis was performed using Prism 7.0 (GraphPad Software).

Results

As a first question, we asked whether and how the developmental time course of KCC2 expression differed between somatosensory cortex and hippocampus. To evaluate overall expression levels, we performed western blot and measured both the monomeric (140KDa) and dimeric (~250–280KDa) forms of KCC2 at 3 developmental ages, P0, P7, and P14. Consistent with previous studies (Markkanen et al. 2014), we found that KCC2 expression levels were low at P0 and increased over the first 2 postnatal weeks, in both brain regions (Fig. 1A,B, Suppl. Fig. S1; 2-way ANOVA, factor age: $^{***}P < 0.0001$ for both KCC2 monomer and dimer bands). We found no overall statistical difference in KCC2 expression between the hippocampus and the somatosensory cortex at all ages examined (Fig. 1B; 2-way ANOVA, KCC2 monomer: factor brain region: $P = 0.0549$, interaction: $P = 0.3030$; KCC2 dimer: factor brain region: $P = 0.1342$, interaction $P = 0.4073$). KCC2 protein can be found both in cytoplasmic and plasmalemmal compartments, but KCC2-dependent Cl^- extrusion in neurons is most dependent on KCC2 expression in the neuronal membrane (i.e., the surface pool). Thus, we asked whether KCC2 localization in the plasmalemmal compartment could be different in those regions. First, we quantified KCC2 levels in the membrane fractions from hippocampus and somatosensory cortex of P7 and P20 pups, by western blot (Fig. 1C,D, Suppl. Fig. S1). We could detect only KCC2 dimers in the membrane fraction, whose expression levels have been previously shown to increase with age and to correlate with the development of inhibitory neurotransmission (Blaesse et al. 2006; Mahadevan et al. 2015). We found that membrane KCC2 levels were significantly higher in the hippocampus compared with the cortex at P7 (Fig. 1D; *t*-test $P = 0.0177$), but not at P20 (Fig. 1D; *t*-test $P = 0.6152$). As a complementary approach, we compared KCC2 immunostaining intensity in pyramidal neuron membranes from the CA1 and layer 2/3 of the somatosensory cortex at P7 (Fig. 1E). KCC2 was already localized along pyramidal soma membranes in the CA1 at P7, but not in the cortex (Fig. 1E,F; Hipp: 84 ± 1%; cortex: 10 ± 1%; *t*-test, $^{*}P < 0.001$). On the other hand, KCC2 could be observed along the membranes of cortical pyramidal neurons by P20, similarly to what observed in CA1 pyramidal neurons (Fig. 1E,G; Fig. 1F, Hipp: 94 ± 2%, cortex: 89 ± 4; *t*-test, $P = 0.270$). Altogether, our results show that, during the first postnatal week, KCC2 localization to the plasmalemmal compartment is much higher in the CA1 region. While cytoplasmic KCC2 may still affect several aspects of neural circuit formation, including glutamatergic synapse formation, it does not seem to affect E_{GABA} (Khalilov et al. 2011); thus, our results suggest that KCC2 transporter activity may play a larger role in influencing E_{GABA} in the hippocampus than in cortex during this developmental time window.

It has been reported that premature KCC2 expression induces a long-term increase in dendritic spine density in somatosensory cortical pyramidal neurons (Fiumelli et al. 2013). However, whether KCC2 premature expression affects spine formation in hippocampal pyramidal neurons in the same fashion is still unknown. To address this question, we overexpressed KCC2 by in utero electroporation at embryonic day 17 (E17) specifically in the CA1 region of the hippocampus, by using a triple-electrode probe (Dal Maschio et al. 2012). We expressed 2 different forms of KCC2, the wild type form (KCC2wt) as well as KCC2 carrying the C568A point mutation (KCC2 C568A), lacking both the cotransporter activity and its binding activity to the protein 4.1 N, which mediates its interaction with the cytoskeleton (Li et al. 2007). KCC2 plasmids were coelectroporated with Td-Tomato to label the entire neuron arborization, while Td-Tomato alone served as a control. Transfected CA1 pyramidal cells were imaged and analyzed at P20 (Fig. 2A). Premature expression of KCC2wt, but not KCC2 C568A, significantly decreased spine density in basal dendrites of CA1 pyramidal cells (Fig. 2B,C; Ctrl: 0.78 ± 0.05 spine/µm; KCC2wt: 0.62 ± 0.04 spine/µm; KCC2-C568A: 0.82 ± 0.08 spine/µm; one-way Anova, $^{*}P = 0.0492$). On the other hand, KCC2 C568A-expressing cells showed significantly longer spines (Fig. 2D; Ctrl: 1.42 ± 0.05 µm, KCC2wt: 1.42 ± 0.05 µm; KCC2-C568A: 1.64 ± 0.03 µm; one-way Anova, $^{*}P = 0.0142$). Longer spines have been suggested to represent immature thin or filopodia spine (Bosch and Hayashi 2011), however, KCC2 mutant expressing cells showed long spines with a distinctive mushroom head, indicating they are likely not immature (Fig. 2B). In fact, spine diameter analysis revealed that KCC2-C568A electroporated pyramidal cells had significantly larger spines compared with Ctrl and KCC2wt electroporated neurons (Fig. 2E; Ctrl: 0.650 ± 0.009 µm, KCC2wt: 0.675 ± 0.003 µm; KCC2-C568A: 0.86 ± 0.01 µm; one-way ANOVA, $^{***}P < 0.0001$). One possibility is that KCC2-C568A may act as a dominant negative, since in utero electroporation of shRNA against KCC2 in CA1 neurons caused a similar increase in spine length (but not spine head size) (Awad et al. 2016).

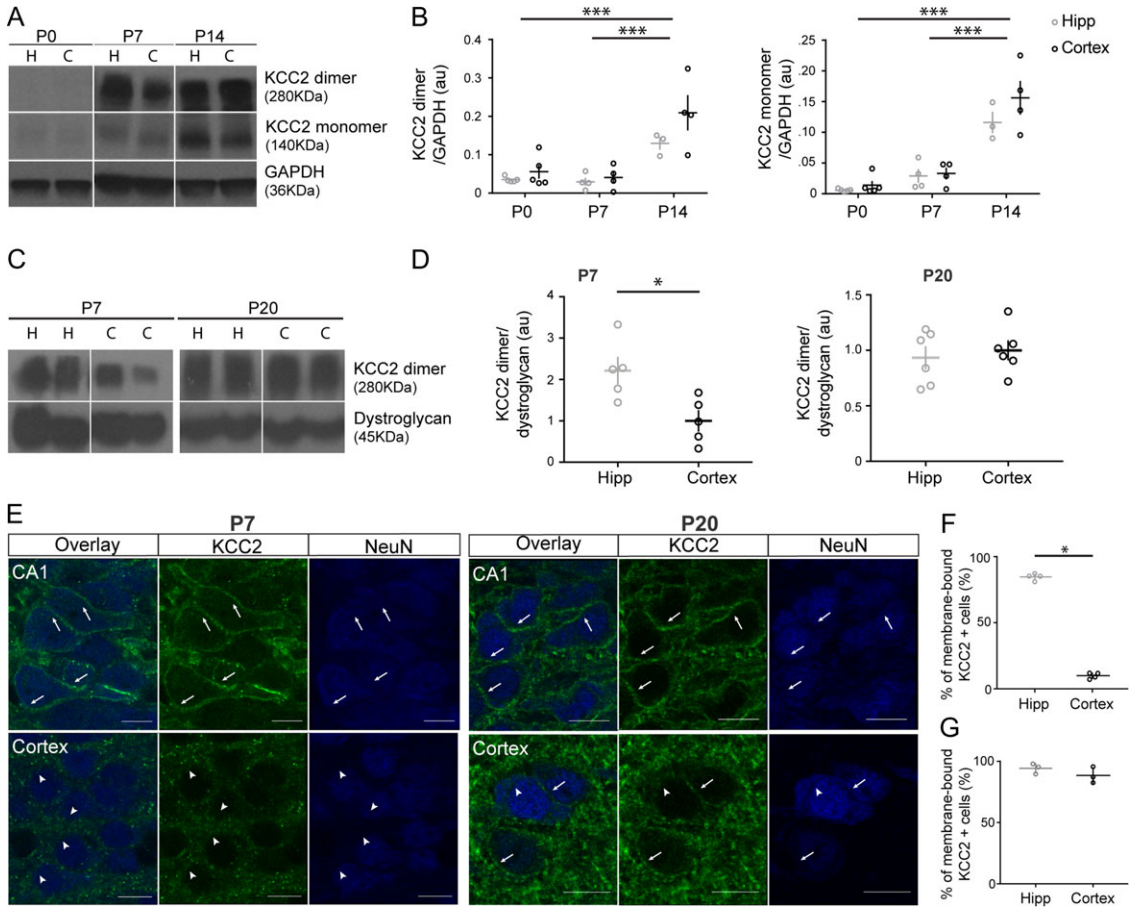

Figure 1. KCC2 localization in the plasmalemmal compartment of pyramidal cell somata occurs earlier in the hippocampus compared with the somatosensory cortex. (*A*) Western blot analysis of KCC2 monomer and dimer expression levels (monomer: 140KDa; dimer: >250KDa) in the hippocampus (H) and cortex (C) extracted from the same animals at different postnatal days (postnatal day 0—P0, P7, and P14). Blot shows representative samples of both regions from one animal per age. (*B*) Quantification reveals that KCC2 expression of the dimer (upper panel) and monomer (lower panel) are not significantly different between brain regions, but significantly increases with time (2-way Anova, KCC2 monomer: brain region, $P = 0.0549$; age, $^{***}P < 0.0001$; KCC2 dimer: brain region, $P = 0.1342$; age, $^{***}P < 0.0001$) P0: $n = 5$ rats, P7: $n = 4$ rats, P14: $n = 4$ rats. Circles represent individual sample values. Horizontal and vertical lines represent mean and SEM, respectively. (*C*) Western blot analysis of KCC2 in the membrane fractions prepared from the hippocampus (H) and cortex (C) extracted from the same animals at P7 and P20. Blot shows representative samples of both regions from 2 animals per age. (*D*) Quantification reveals that the expression of KCC2 dimer is significantly higher in the hippocampus than in somatosensory cortex at P7 (t-test $^{*}P = 0.0177$), but not at P20 (t-test $P = 0.6152$). Note that we did not reliably detect KCC2 monomer in the membrane fractions. P7: $n = 5$ rats, P20: $n = 6$ rats. Circles represent individual sample values. (*E*) Confocal images of KCC2 immunostaining (green) at P7 and P20. Neuronal somata are labeled with anti-NeuN antibody (blue). By P7, KCC2 staining is clearly visible in the plasmalemmal compartment of CA1 (arrows), but not of cortical (arrowheads) pyramidal neurons. Scale bar, 10 μm. (*F*,*G*) Quantification of the percentage of NeuN+ cells showing KCC2 membrane immunostaining at P7 (*F*) and P20 (*G*) (t-test, P7: $^{*}P = 0 < 0.001$; P20: $P = 0.270$).

Since the effects of KCC2 premature expression we observed in the hippocampus were the opposite to what were previously reported for the somatosensory cortex (Fiumelli et al. 2013), we sought to verify that our results were not due to technical differences, by electroporating the same constructs described above in somatosensory cortex (Fig. 2A,F). Consistently with previous studies (Fiumelli et al. 2013), we found that KCC2wt premature expression caused spine density increase (Fig. 2F,G, Ctrl: 1.41 ± 0.12 μm; KCC2wt: 2.17 ± 0.17 μm; one-way Anova, $^{**}P = 0.005$). KCC2-C568A expression, on the other hand, did not affect spine density (Fig. 2G, Tukey's multiple comparison Ctrl vs. KCC2 C568A mutant $P = 0.372$), or head size (Fig. 2G–I, Tukey's multiple comparison Ctrl vs. KCC2 C568A mutant $P = 0.914$), while it only had a minor effect on spine length (Fig. 2H, Tukey's multiple comparison Ctrl vs. KCC2 C568A mutant $P = 0.212$; K–S test Ctrl vs. KCC2-C568A $^{**}P = 0.0006$).

In utero electroporation introduced KCC2 in many, neighboring pyramidal neurons (Fig. 2A), thus, potentially affecting the local network excitability by rendering E_{GABA} more negative in densely transfected neurons (Cancedda et al. 2007). Therefore, we asked whether the opposite effects of KCC2 premature expression in CA1 and somatosensory pyramidal neurons were due to cell autonomous or circuit-based effects. To address this question, we transfected KCC2wt in isolated pyramidal cells in either hippocampal or cortical organotypic cultures, by biolistic transfection, from equivalent postnatal day (EP) 6 to EP20 (Fig. 3A). Similarly to what was observed following in utero-electroporation in vivo (Fig. 2B,C), KCC2wt transfected CA1 neurons displayed a significant decrease in spine density compared with control pyramidal neurons (Fig. 3B–D, Ctrl: 0.99 ± 0.12 spine/μm; KCC2wt: 0.56 ± 0.05 spine/μm; t-test $^{**}P = 0.0083$). In contrast, spine length and spine head diameter were not significantly affected in KCC2wt-expressing neurons compared with controls (Fig. 3E, t-test $P = 0.2248$; Fig. 3F; t-test $P = 0.5903$). We then performed the same experiment in cortical organotypic cultures. Similarly to what we observed in vivo

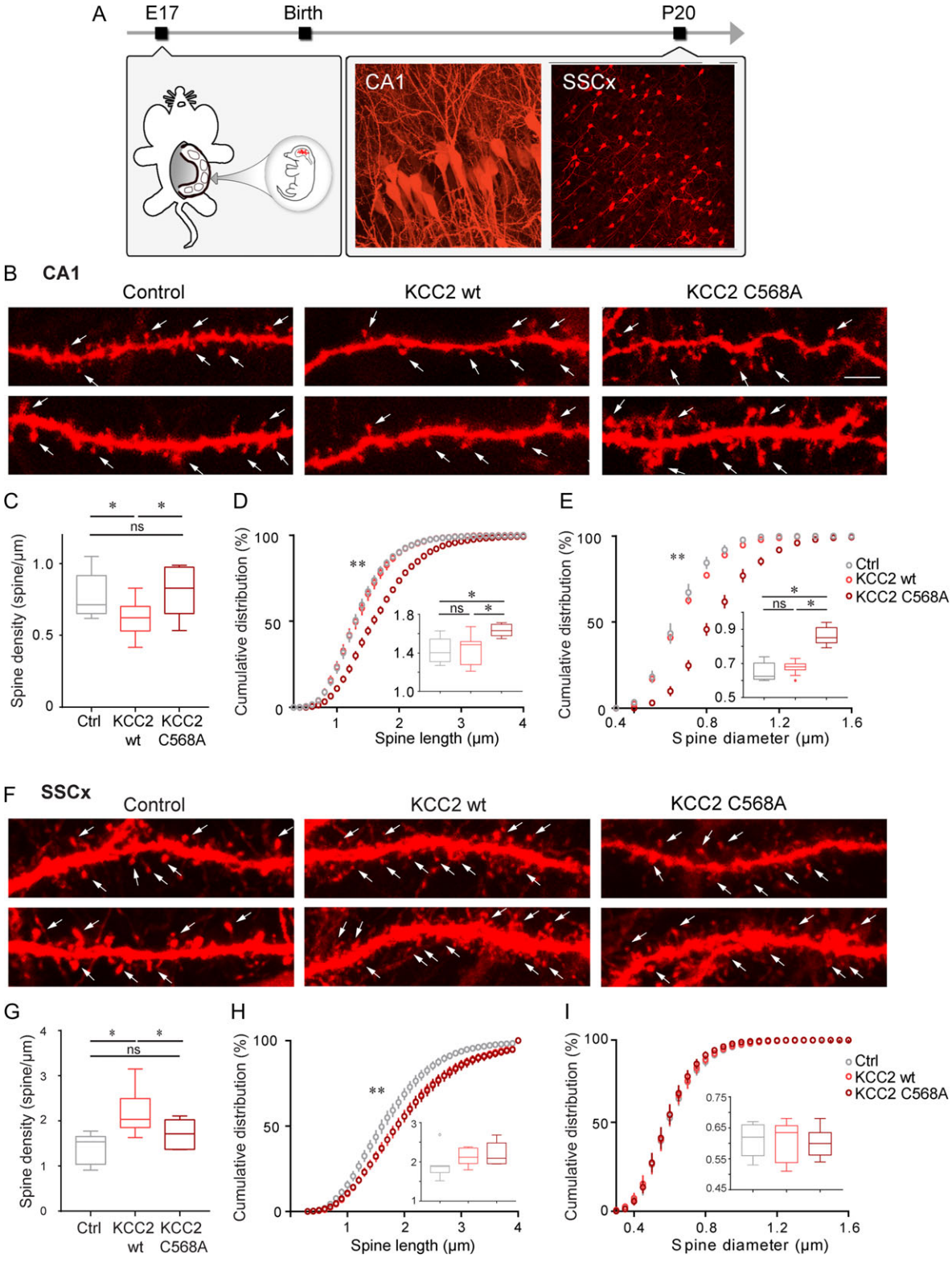

Figure 2. Premature expression of KCC2 in vivo decreases spine density in hippocampal neurons, but increases spine density in cortical pyramidal neurons. (*A*) Schematics of experimental procedure. (*B*) Representative basal dendrite segments from 2 different CA1 pyramidal cells showing that KCC2wt-expressing cells have fewer spines, while KCC2mut have longer and larger spines compared with control cells. Arrows indicate spines. Scale bar, 5 µm. (*C*) Spine density is significantly reduced in KCC2wt-expressing cells compared with control and KCC2 C568A-expressing ones (one-way Anova, $^{*}P = 0.0492$). (*D*, *E*) Cumulative distribution and average (inset) spine length (*D*) and spine diameter (*E*). (*D*: one-way Anova $^{*}P = 0.0142$; Kolmogorov–Smirnov (KS) test, Ctrl vs. KCC2wt $^{*}P = 0.0147$; Ctrl vs. KCC2-C568A $^{***}P < 0.0001$; KCC2wt vs. KCC2-C568A $^{***}P < 0.0001$; *E*: one-way Anova, $^{***}P < 0.0001$; K–S test, Ctrl vs. KCC2-C568A $^{**}P = 0.0002$; KCC2wt vs. KCC2-C568A $^{**}P = 0.0091$). Pyramidal neurons: Ctrl, $n = 8$ from 5 animals, KCC2wt, $n = 9$ from 5 animals, KCC2-C568A, $n = 5$ from 3 animals. (*F*) Confocal images showing representative basal dendrite segments of pyramidal neurons from somatosensory cortex. (*G*–*I*) Analysis of spine density (*G*), spine length (*H*), and spine diameter (*I*) of cortical pyramidal

(Fig. 2F,G), we found that KCC2 premature expression in the cortex induced a striking increase in spine density of pyramidal cells (Fig. 3G–I, Ctrl: 0.91 ± 0.08 spine/µm; KCC2wt: 1.76 ± 0.1 spine/µm; *t*-test, ***$P < 0.0001$), as well as an increase in spine length (Fig. 3J, 1.58 ± 0.05 spine/µm; KCC2wt: 1.76 ± 0.04 spine/µm; *t*-test, *$P = 0.0238$) while there were no statistical difference in spine diameter (Fig. 3K, *t*-test, $P = 0.7203$). Altogether, these results confirm that premature overexpression of KCC2 leads to a decrease of spine density of CA1 pyramidal neurons; while it leads to an increase in spine density in cortical layer 2/3 pyramidal cells, both in vivo and in vitro. Further, this effect is cell autonomous, as low-density overexpression of KCC2 in organotypic cultures showed similar results as high-density KCC2 electroporation in vivo.

BDNF can increase KCC2 activation, by regulating its localization at the membrane, in the developing brain (Khirug et al. 2010; Puskarjov et al. 2015). Could a difference in BDNF expression in CA1 versus cortex affect KCC2 localization? To answer this question, we first performed a western blot analysis of BDNF expression levels in the hippocampus compared with the somatosensory cortex, both in vivo and in vitro. In vivo, we found significantly higher levels of BDNF in the hippocampus than in the cortex extracted from the same animal at P7 and P14 (Fig. 4A; 2-way Anova, age ***$P < 0.0001$, brain region ***$P < 0.0001$, interaction ***$P < 0.0001$—Sidak's multiple comparison P7: *$P = 0.0144$, P14: ***$P < 0.0001$), while we found no difference at P0 (Fig. 4A; Sidak's multiple comparison test, $P > 0.9307$). In vitro, we collected the first data point at EP8, 2 days after culture preparation, since we have previously observed that 2 days are needed for the slices to attach to the membranes and to eliminate most cellular debris caused by slicing. The variability in BDNF expression levels between different samples was more pronounced in vitro than in vivo, nevertheless we found that BDNF levels were significantly higher in the hippocampal cultures compared with cortical cultures at EP8, while they showed a tendency towards higher values at EP12 (Fig. 4B; 2-way Anova, age, $P = 0.0521$, brain region, **$P = 0.0026$, interaction *$P = 0.0566$). Thus, these data suggest that, both in vivo and in vitro, BDNF expression levels are higher in the hippocampus compared with the cortex during the first 2 postnatal weeks.

To understand whether this difference in BDNF levels may contribute to the region-specific effects of KCC2 premature expression on spine formation, we increased BDNF in cortical organotypic cultures by adding it (50 ng/mL) to the culture medium (Fig. 4C). We predicted that if the ability of KCC2 premature expression to increase pyramidal cell spine density were due to the lower levels of BDNF, pyramidal neurons transfected with KCC2wt would show no increase, or even a decrease, in spine density compared with control neurons, in cortical cultures treated with BDNF. Indeed, we found no statistical difference in spine density between untreated control pyramidal neurons, pyramidal neurons treated with BDNF or pyramidal neurons transfected with KCC2wt and treated with BDNF (Fig. 4D,E; Ctrl: 0.91 ± 0.08 spine/µm; Ctrl + BDNF: 1.18 ± 0.09 spine/µm; KCC2wt + BDNF: 1.27 ± 0.13 spine/µm; one-way Anova, $P = 0.0765$). BDNF treatment induced a slight increase in spine length in control pyramidal neurons (one-way Anova, *$P = 0.0366$), but had no major effect on spine diameter (one-way Anova, $P = 0.1047$). In contrast to what was previously reported in hippocampal organotypic cultures (Tyler and Pozzo-Miller 2001, 2003), we did not find an increase in spine density in BDNF-treated cortical organotypic cultures, a difference that might be explained by the different medium composition, BDNF concentration and length of BDNF treatment (Kellner et al. 2013). Nonetheless, our data show that KCC2 premature expression is unable to increase spine density in cortical pyramidal neurons in the presence of higher BDNF levels.

Next, we investigated whether KCC2 expression and/or localization were affected by BDNF treatment. Since the difference in KCC2 plasmalemmal localization in pyramidal neurons between CA1 and somatosensory cortex was clearly visible at P7, but not overly different by P20 (Fig. 1C–G; Suppl. Fig. S1), we analyzed KCC2 expression and localization at EP9, after 5 days of treatment with BDNF. As expected, western blot analysis revealed no statistical difference in overall KCC2 expression levels (Fig. 5A,B, KCC2 monomer, *t*-test $P = 0.7829$; KCC2 dimer, Mann–Whitney test $P = 0.3929$); we thus analyzed KCC2 plasmalemmal localization by immonolabeling (Fig. 5C, D) and western blot analysis of membrane fractions (Fig. 5E,F; Suppl. Fig. S1). Immunofluorescence analysis revealed that KCC2 expression at the membrane of pyramidal cell somata was significantly increased by BDNF treatment (Fig. 5C,D; *t*-test, *$P = 0.0359$). Quantification of KCC2 in the membrane fractions showed that variability in KCC2 expression levels between different samples was more pronounced in vitro than in vivo, nevertheless, when comparing cultures prepared from the same pup, we found that membrane KCC2 levels were significantly higher in organotypic cultures treated with BDNF compared with those untreated (Fig. 5E,F; paired *t*-test *$P = 0.0143$). Therefore, both experimental approaches indicate that BDNF strongly promotes the localization in the plasmalemmal pool of already synthetized KCC2.

Higher BDNF expression levels may be responsible for the pronounced KCC2 localization at the membrane of CA1 pyramidal neurons during the first 2 postnatal weeks, which in turn might affect spine formation. In particular, more pronounced KCC2 localization at the membrane could translate into a larger role for KCC2 transporter function in this specific developmental window. In the somatosensory cortex, Fiumelli et al. (2013) reported that the increase of spine density due to premature KCC2 expression was ion-transport independent, since electroporation of 2 transporter-inactive KCC2 variants, the C-terminal domain of KCC2 (KCC2 CTD), and the N-terminal deleted form of KCC2 (KCC2 ΔNTD) induced an increase in pyramidal cell spine density that was undistinguishable from that induced by electroporation of KCC2wt. In the CA1 region of the hippocampus, we found that, while premature expression of KCC2wt decreased spine density (Fig. 2B,C), both KCC2 CTD and KCC2 ΔNTD had no affect on spine density compared with control pyramidal cells (Fig. 6A,B; Ctrl: 1.36 ± 0.06 spine/µm; KCC2 CTD: 1.31 ± 0.10 spine/µm; KCC2 ΔNTD: 1.38 ± 0.05 spine/µm; one-way Anova, $P = 0.8019$). KCC2 CTD induced a slight increase of spine length (Fig. 6C; Ctrl: 1.26 ± 0.03 µm; KCC2 CTD: 1.40 ± 0.04 µm; KCC2 ΔNTD 1.26 ± 0.03 µm; one-way Anova, *$P = 0.0129$), but no difference in spine diameter (Fig. 6D; one-way Anova, $P = 0.1301$). These results suggest that the transporter

neurons reveals that KCC2wt premature expression increases spine density (one-way Anova, **$P = 0.005$), but neither spine length (one-way Anova, $P = 0.193$) or spine diameter were affected (one-way Anova, $P = 0.921$). Cumulative distribution of spine length shows slightly longer values in KCC2wt and KCC2 C568A transfected cells (KS test: Ctrl vs. KCC2wt **$P = 0.0006$; Ctrl vs. KCC2-C568A **$P = 0.0006$; KCC2wt vs. KCC2-C568A $P > 0.99$). Pyramidal neurons: Ctrl: $n = 7$ from 3 animals, KCC2wt: 8 from 5 animals, KCC2 C568A: 6 from 3 animals.

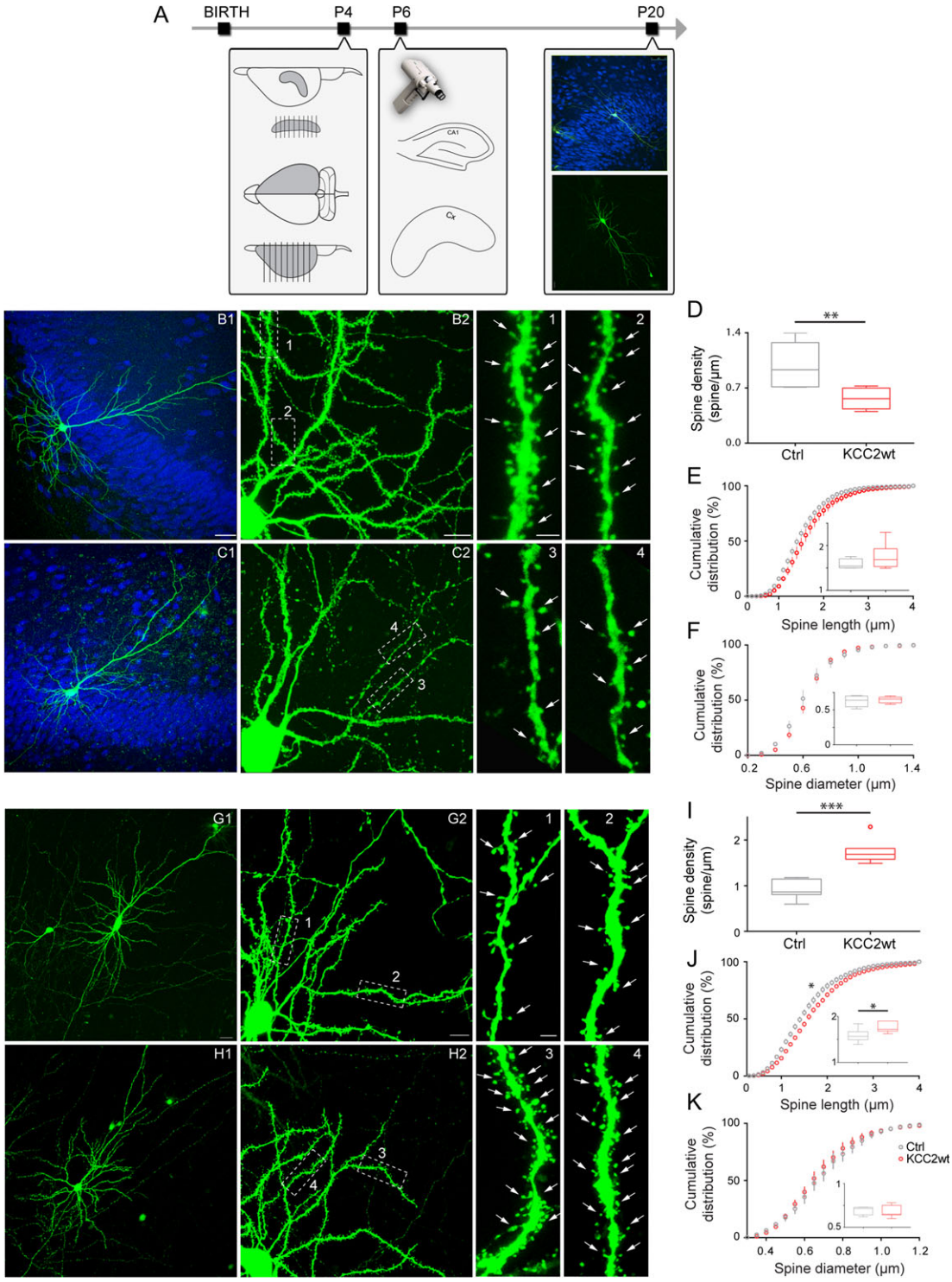

Figure 3. The effects of KCC2 premature expression on spine density are cell-autonomous. (*A*) Schematics of experimental procedure. (*B*,*C*) Low (B1,C1) and high (B2, C2) magnification of CA1 transfected pyramidal cells (NeuN immunostaining, blue). KCC2wt-expressing cells show fewer spines (3–4, arrowheads) compared with control cells (1–2, arrowheads). The 1–4 are from boxed regions in B2, C2. Scale bars B1–C1, 50 µm; B2–C2, 10 µm; b1/2–c3/4, 2 µm. (*D*) Spine density is strongly reduced in KCC2wt-overexpressing cells (*t*-test, $^{*}P = 0.0083$). (*E*,*F*) Cumulative distribution and average (inset) spine length (*E*) and spine diameter (*F*) (*E*: *t*-test, $P = 0.2248$; K–S test, $P = 0.4070$; *F*: *t*-test, $P = 0.5903$; K–S test, $P = 0.9957$). $n = 6$ Ctrl pyramidal cells, $n = 6$ KCC2 wt pyramidal cells. (*G*,*H*) Low (G1,H1) and high (G2,H2) magnification of cortical pyramidal neurons. Spine density is increased in KCC2wt-overexpressing cells (compare dendrite segment in 3–4 with those in 1–2). Scale bars G1–H1, 50 µm; G2–H2, 10 µm; g1/2–h3/4, 2 µm. (*I*) Spine density (*t*-test, $^{***}P < 0.0001$). (*J*) Spine length (*t*-test, $^{*}P = 0.0238$; K–S test, $^{*}P = 0.0116$). (*K*) Spine diameter (*t*-test, $P = 0.7203$; K–S test, $P = 0.3075$). $n = 7$ Ctrl cells, $n = 7$ KCC2wt-transfected cells.

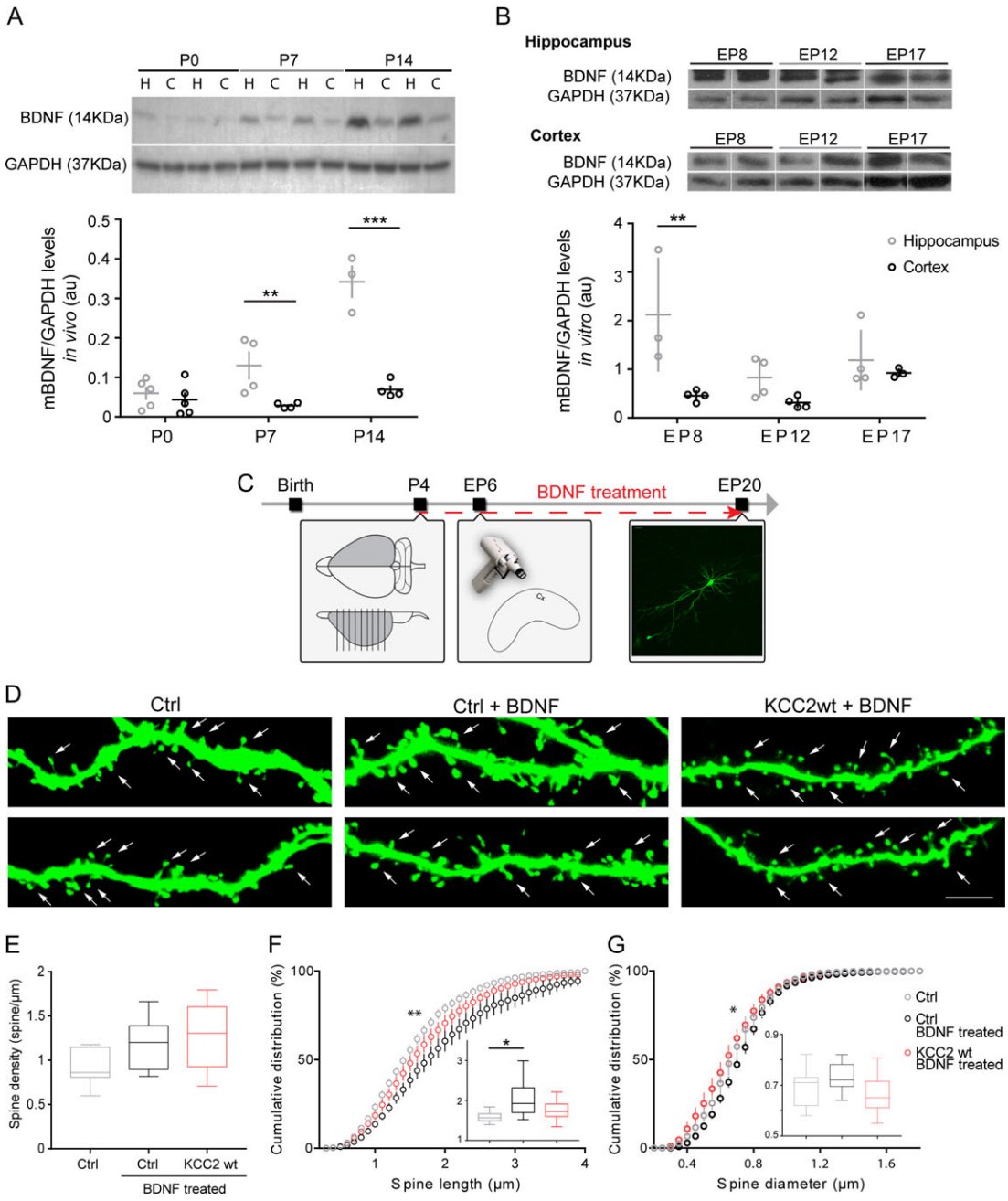

Figure 4. BDNF treatment blocks the spinogenesis promoting effect of KCC2 premature expression. (*A*) Western blot representative bands (top) and analysis (bottom) of BDNF protein levels in vivo reveal that BDNF expression is higher in the hippocampus than in the cortex during the first postnatal weeks (2-way Anova, age, $^{***}P < 0.0001$, brain region, $^{***}P < 0.0001$). Hippocampus: $n = 5$, 4, and 3 for P0, P7, and P14, respectively; Cortex: $n = 5$, 4, and 4 for P0, P7, and P14, respectively. *N* represents number of rats. (*B*) Western blot analysis of organotypic cultures shows that BDNF levels are higher in hippocampal than in cortical cultures during the first postnatal week in organotypic cultures (2-way Anova, age $P = 0.0521$, brain region $^{**}P = 0.0024$). Hippocampus: $n = 3$, 4, and 4 for P8, P12, and P17, respectively; Cortex: $n = 4$, 4, and 3 for P8, P12, and P17, respectively. *N* represents samples, where each sample is obtained by pooling 3–4 cultured slices together. (*C*) Schematic of experimental procedure. (*D*) Representative basal dendrite segments of pCI-GFP transfected cortical pyramidal neurons, either untreated (Ctrl), or treated with BDNF (Ctrl + BDNF), and of pCI-GFP/KCC2wt transfected pyramidal neurons treated with BDNF (KCC2wt+BDNF). (*E*) Spine density analysis (one-way Anova, $P = 0.0765$). (*F*) Cumulative and average (inset) spine length analysis reveal that spines are longer after BDNF treatment, independently of KCC2 overexpression (one-way Anova, $P = 0.0366$; K–S test, Ctrl vs. Ctrl + BDNF $^{**}P = 0.0003$, Ctrl vs. KCC2wt + BDNF $P = 0.0707$; Ctrl + BDNF vs. KCC2wt + BDNF $^{*}P = 0.0365$). (*G*) Cumulative and average (inset) spine diameter analysis (one-way Anova, $P = 0.1047$; K–S test: Ctrl vs. Ctrl + BDNF $^{*}P = 0.0413$; Ctrl vs. KCC2wt + BDNF $P = 0.2877$; Ctrl + BDNF vs. KCC2 wt + BDNF $^{*}P = 0.0164$). $N = 7$ Ctrl cells; $n = 9$ ctrl+BDNF cells; $n = 9$ KCC2wt + BDNF cells.

function of KCC2 contributes to the effects of KCC2 on spine formation in the hippocampus during the first postnatal weeks, possibly due to its more pronounced localization at the membrane.

All together our data demonstrate that the effects of KCC2 premature expression on spine formation are brain-region specific, and in particular, may be dependent on the local levels of BDNF.

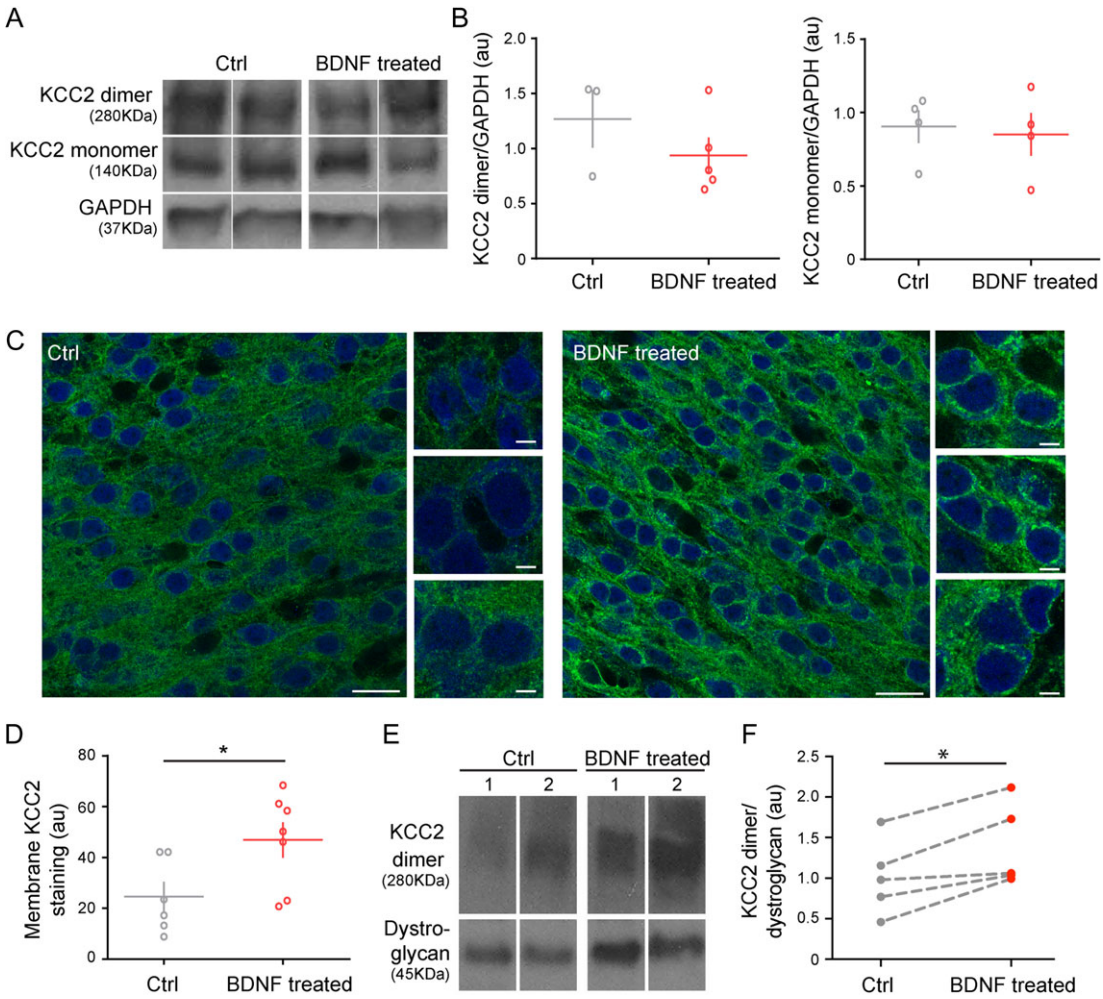

Figure 5. BDNF treatment in organotypic cortical cultures increases KCC2 expression levels in the plasmalemmal compartment. (*A*, *B*) Example bands (*A*) and quantification (*B*) of western blot analysis of KCC2 expression in cortical organotypic cultures either untreated or treated with BDNF (monomer: *t*-test, $P = 0.7829$, dimer: Mann Whitney test $P = 0.3929$). $n = 4$ Ctrl and $n = 4$ BDNF-treated samples (4 organotypic cultures are pooled together for each sample). (*C*) Representative images of KCC2 immunostaining (green) and quantification (*D*) of cortical organotypic cultures either untreated (Ctrl) or treated with BDNF. Neuronal somata are immunostained with NeuN (blue). Scale bar, 50 μm; inset scale bar, 5 μm. *t*-test, $^*P = 0.0359$; $n = 66$ neurons from $N = 6$ Ctrl slices, and $n = 77$ neurons from $N = 7$ BDNF-treated slices. Graphs represent mean ± SEM, with *N* of slices as independent replicates. (*E*) Example bands of western blot analysis of KCC2 expression in membrane fractions prepared from cortical organotypic cultures either untreated or treated with BDNF. Numbers (1,2) indicate cultures prepared from the same pup. (*F*) Quantification shows that BDNF treatment significantly increases membrane levels of KCC2 (paired *t*-test $^*P = 0.0143$). $N = 5$ animals.

Discussion

The main finding of our work is that premature KCC2 expression, during the same developmental time window, has 2 distinct and opposite effects on spine formation in CA1 region of the hippocampus and in the overlying somatosensory cortex, 2 structures that are often considered similar when synapse formation mechanisms are tackled. In particular, we demonstrate that the effects of KCC2 premature expression on spine formation in CA1 are dependent on the transporter activity, contrary to what was reported in cortical neurons (Li et al. 2007; Fiumelli et al. 2013). Finally, our findings suggest caution is necessary before generalizing molecular mechanisms regulating synapse formation to different brain regions.

Why do cortical and CA1 pyramidal cells respond so differently to increased KCC2 expression? KCC2 function is not solely determined by its expression levels; in fact, KCC2 proteins can be found both in cytoplasmic and plasmalemmal pools, and the relative abundance of these 2 pools could change depending on the age and activity levels in the network (Khirug et al. 2010; Khalilov et al. 2011; Puskarjov et al. 2015). Regulation of KCC2 membrane localization likely allows for finer tuning and rapid changes of Cl^- gradients. Therefore, KCC2 levels in the plasmalemma pool might be a better indicator of the impact of KCC2 transporter function on E_{GABA} compared with the total levels of KCC2 protein. For example, despite similar high expression levels of KCC2 protein during the first postnatal month, the capacity to extrude Cl^- in neurons of the lateral superior olive emerges gradually during the first 2 postnatal weeks (Balakrishnan et al. 2003). Our results show that the relative abundance of the plasmalemmal and the cytoplasmic KCC2 pools is temporally and spatially heterogeneous, even when comparing regions that are developmentally and ontogenetically very close as the hippocampus and the cortex. Indeed, while we did not detect any difference in the time course of KCC2 expression increase between the hippocampus and the somatosensory cortex, we found that membrane KCC2 levels were at least 2-fold higher in the hippocampus than in the cortex, in P7 rats. Additionally, we could detect KCC2

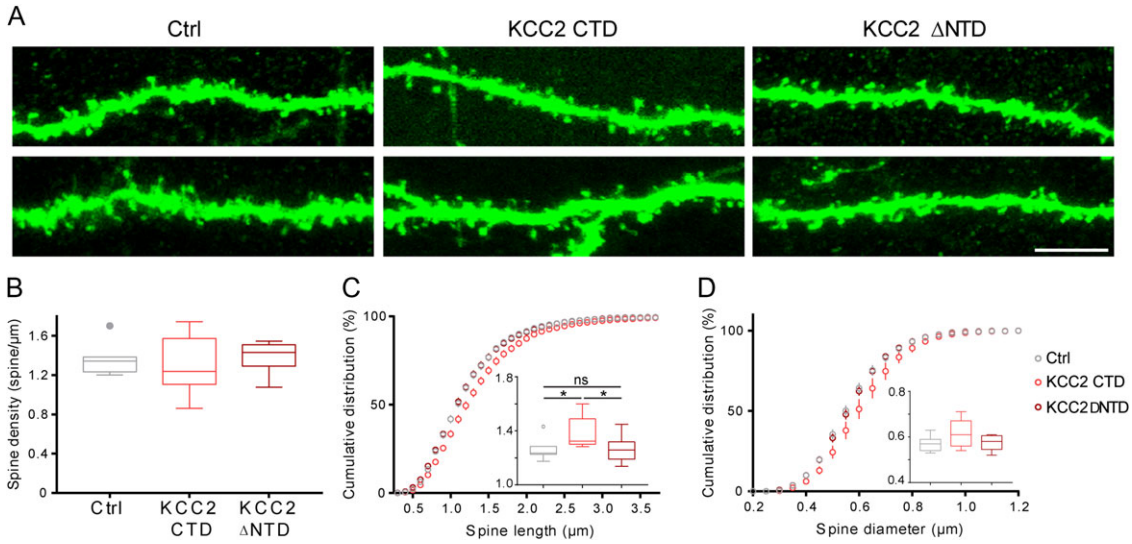

Figure 6. Transporter-dead KCC2 mutants are unable to induce spine loss in CA1 pyramidal neurons. (*A*) Confocal images of basal dendrites from 2 different pyramidal neurons per experimental groups, in utero electroporated with pCI-GFP alone or pCI-GFP together with C-terminal region of KCC2 (KCC2 CTD) or the N-terminal deleted KCC2 mutant (KCC2 ΔNTD). Scale bar, 5 µm. (*B*) Spine density is not significantly different between the 3 groups (one-way Anova, $P = 0.8019$). (*C*) Cumulative and average (inset) spine length show longer spines in KCC2 CTD transfected neurons (one-way Anova, $^*P = 0.0129$; K–S test, Ctrl vs. KCC2 CTD $P = 0.0707$, Ctrl vs. KCC2 ΔNTD $P = 0.07532$, KCC2 CTD vs. KCC2 ΔNTD $^*P = 0.0234$). (*D*) Cumulative and average (inset) spine diameter analysis reveal no significant difference between the 3 groups (one-way Anova, $P = 0.1301$; K–S test, Ctrl vs. KCC2 CTD $P = 0.4401$, Ctrl vs. KCC2 ΔNTD $P = 0.9925$; KCC2 CTD vs. KCC2 ΔNTD $P = 0.2264$). Ctrl: $n = 7$ pyramidal cells from 3 animals; KCC2 CTD: $n = 9$ pyramidal cells from 4 animals; KCC2 ΔNTD: $n = 9$ KCC2 NTD pyramidal cells from 4 animals.

immunolabeling in the plasmalemmal of close to 100% of CA1 pyramidal neurons, but only in 10% of somatosensory pyramidal neurons, at the same age (Fig. 1). However, the difference in the localization of KCC2 immunolabeling or in membrane KCC2 levels between the 2 brain regions was negligible by P20 (Fig. 1). These observations suggest that KCC2 may play a stronger role in regulating E_{GABA} in CA1 than in cortical pyramidal neurons, at least during the first postnatal week. To be able to clearly detect plasmalemmal KCC2 localization in situ, we focused on the somatic compartment of pyramidal cells. However, it is important to note that KCC2 membrane expression profiles could be in principle distinct in various subcellular structures in neurons, since several studies have shown differences in E_{GABA} between the dendritic, somatic, and axon initial segment compartments (Duebel et al. 2006; Baldi et al. 2010; Rinetti-Vargas et al. 2017).

During neural circuit formation, synapse number is regulated both by genetic and activity-dependent mechanisms. In this context, we could envision the battling of 2 actions induced by KCC2 overexpression, the spinogenesis promoting effects, mediated by changes in cytoskeleton dynamics (Li et al. 2007; Gauvain et al. 2011; Fiumelli et al. 2013; Chevy et al. 2015), and the transporter-mediated alteration of GABA driving force. Premature expression of KCC2 leads to more negative E_{GABA} (Rivera et al. 2004; Cancedda et al. 2007; Galanopoulou 2008; Khirug et al. 2010; Pellegrino et al. 2011), which may render spike generation and back-propagating action potentials less likely. Reduced neuronal activity may in turn impair synapse potentiation, therefore leading to synaptic loss (Turrigiano et al. 1998). Since we observed that, at P7, KCC2 immunolabeling is already clearly visible in the plasmalemmal compartment in CA1, but not cortical, pyramidal neurons, and membrane KCC2 levels are significantly higher in the hippocampus compared with the cortex, it is possible that KCC2 premature expression may have a larger impact on E_{GABA} in CA1 hippocampal neurons, therefore leading to impaired spine formation/stabilization. Further studies are needed to clarify to what extent E_{GABA} differs between pyramidal cells in CA1 and in the somatosensory cortex during the first postnatal weeks.

One possibility is that the effects of KCC2 premature expression on spinogenesis may be secondary to global alterations of neuronal activity caused by widespread alterations in E_{GABA}, which may occur following high-density in utero electroporation of KCC2 cDNA. We think that this is unlikely because single-cell KCC2 overexpression in CA1 pyramidal neurons in hippocampal and cortical organotypic cultures induced dendritic spine alterations similar to those observed following in utero electroporation in vivo. In our hands, biolistic transfection leads to plasmids expression in only few (>5), sparse pyramidal cells per organotypic culture, which is unlikely to perturb network activity. Therefore, it seems more likely that it is the specific cellular contexts in which the transfected neurons develop that determine how KCC2 overexpression affects spine formation.

What are the molecular mechanisms underlying the different effects of premature KCC2 expression in cortical versus CA1 pyramidal neurons? BDNF is one the strongest modulator of KCC2 activity (Rivera et al. 2002; Kaila, Price, et al. 2014). Most importantly, this modulation is age-dependent as BDNF accelerates KCC2 expression and its phosphorylation-mediated activation in developing neurons in normal condition or following seizures (Fiumelli et al. 2005; Fiumelli and Woodin 2007; Khirug et al. 2010; Ludwig et al. 2011; Puskarjov et al. 2015), while it has the opposite effects in adult neurons following injury, trauma or seizures (Rivera et al. 2002, 2004; Kaila, Price, et al. 2014). Here, we report that overall BDNF expression levels are consistently higher in the hippocampus than in the cortex, extracted from the same animal, during the first 2 postnatal weeks (Fig. 4A). Lower cortical BDNF levels might contribute to the reduced plasmalemmal localization of KCC2 immunostaining, since BDNF has been shown to promote KCC2 confinement at the membrane (Ludwig et al. 2011; Puskarjov et al. 2015). Consistently, treating cortical organotypic cultures with BDNF

lead to significantly increased levels of membrane KCC2, as detected by western blot, and stronger KCC2 immunolabeling in the plasmalemmal compartment of cortical pyramidal somata, in situ (Fig. 5). On the other hand, we did not observe an overall increased KCC2 expression levels in BDNF-treated cultures, in contrast to what previously reported in dissociated cultures (Ludwig et al. 2011). Length of treatment or differences in culture conditions (dissociated neurons vs. organotypic cultures) might contribute to the observed differences. Of note, when treated with BDNF, cortical pyramidal neurons prematurely expressing KCC2 did not show any difference in spine density compared with control neurons, either untreated or treated with BDNF (Fig. 4). Therefore, KCC2 premature expression promotes spine formation only in presence of low BDNF.

Altogether, our data support the hypothesis that BDNF levels modulate the effects of KCC2 on spine formation, at least during the first postnatal weeks. It has been proposed that, in mature hippocampal neurons, KCC2 regulate AMPA receptor clustering in the postsynaptic membranes (Gauvain et al. 2011; Chamma et al. 2013; Chevy et al. 2015). Since BDNF expression is strongly regulated by neuronal activity, in particular by LTP-inducing stimulation, and it is, in turn, important for LTP expression (Patterson et al. 1992; Korte et al. 1996), it will be interesting to investigate whether BDNF levels may also affect directly KCC2-induced AMPA receptor clustering, by modulating KCC2 localization at the membrane. Premature expression of BDNF in pyramidal cells accelerated the development of GABAergic synapses and the onset and closure of critical period plasticity in visual cortex (Huang et al. 1999). Our data suggest that BDNF may exert these effects in part by promoting membrane localization of KCC2, which may in turn increase KCC2 impact on the regulation of intracellular [Cl^-], thus leading to more negative E_{GABA} and more efficient inhibition. Since the timing of critical periods is different between different cortical areas, it will be interesting to explore whether the shift of KCC2 localization from the cytoplasmic to the plasmalemmal compartments will also be similarly different.

We recently reported that electroporation of shRNA against KCC2 at E17.5 induced a reduction of spine density in CA1 pyramidal neurons (Awad et al. 2016). On a first glance, this observation may appear discordant with the data presented here; showing that KCC2 overexpression by the same technique during the same developmental period also causes spine loss. Using shRNA-mediated manipulation and KCC2-deficient mice, a recent study showed that KCC2 interacts with and inhibits β-PIXb, a GEF for small GTPases Rac1 and Cdc42, in hippocampal dissociated cultures (Llano et al. 2015). β-PIX, through activation of Rac1, forms part of the signaling cascade controlling cofilin-1 phosphorylation (Saneyoshi et al. 2008; Mizuno 2013). Rac1 and cofilin-1 are known to play a pivotal role in spine morphogenesis. Interestingly, the activity of these 2 proteins must be tightly regulated to obtain normal spine formation. For example, knockdown of cofilin-1 by shRNA and overexpression of constitutively active cofilin-1 induces similar phenotype in developing neurons: long filopodia-like structures (Hotulainen et al. 2009; Shi et al. 2009). Similarly, both long-term increase and decrease of Rac1 activity leads to decreased spine numbers (Nakayama et al. 2000; Zhang et al. 2003). In other words, the shift in actin turnover balance in either direction results in disrupted dendritic spine development. Therefore, either reducing or increasing KCC2 expression may alter the ratio between active and inactive forms of β-PIX, which in turn would alter both Rac1 and cofilin-1. It remains to be determined to what extent the molecular mechanisms linking KCC2 to cytoskeleton rearrangements are spatially and temporally similar in different brain regions. To add another layer of complexity, it is likely that by reducing KCC2 expression in CA1 pyramidal neurons, we may affect 2 parallel processes, which can potentially affect spine formation in 2 different directions, by promoting the ability of the transfected cells of producing back-propagating potentials and favoring LTP, but at the same time by impairing AMPA receptor aggregation in mature spines (Gauvain et al. 2011; Chevy et al. 2015) that could in turn lead to spine loss. Thus, the balance of these processes will likely determine spine numbers in CA1 pyramidal neurons during development.

Our data show that overexpression of KCC2 C568A, which may act as dominant negative (Pellegrino et al. 2011), by in utero electroporation in the hippocampus significantly increased both spine length and size, without affecting spine density. In addition, overexpression of KCC2-CTD in hippocampal pyramidal neurons in vivo also increased spine length, without affecting spine density (Fig. 6C), consistent to what reported by Li et al. (2007) in cultured neurons. Since KCC2-CTD retains its ability to bind to cytoskeleton proteins, these data support the hypothesis that KCC2 can influence spine morphology independently of its transporter activity, while spine formation may be modulated by both KCC2 transporter activity and its interactions with cytoskeleton proteins when extracellular signals, such as BDNF, promote KCC2 membrane localization and activity. Given that spine length inversely correlates with the spine's contribution to somatic voltage (Araya et al. 2014), dynamic, subcellular changes in KCC2 localization may contribute to synaptic transduction and plasticity by regulating spine neck length.

Recently, several studies, including ours, showed that insults in the developing brain, such as seizures or cortical dysplasia (Galanopoulou 2008; Khirug et al. 2010; Awad et al. 2016), induce a premature expression and/or activation of KCC2. Overall, our results suggest that these pathology-induced alterations of KCC2 expression may differentially affect the formation of dendritic spines in different brain regions. It will be important to understand whether and how these specific circuit alterations are long-lasting and may affect diverse cognitive functions.

Supplementary Material

Supplementary material is available at *Cerebral Cortex* online.

Funding

The Canadian Institutes of Health Research (L.C. and G.D.C.), Canada Foundation for Innovation (G.D.C.), Savoy Foundation (L.C. and G.D.C.). P.N.A. was supported by Savoy Foundation and Fondation CHU Sainte-Justine.

Notes

We would like to thank the Comité Institutionnel de Bonne Pratiques Animales en Recherche (CIBPAR) and all the personnel of the animal facility of the Research Center of CHU Sainte-Justine (Université de Montreal) for their instrumental technical support, Dr Michela Fagiolini for critical discussion and inputs on the article and Dr Christine Vande Velde for her invaluable help with the protocol for membrane extraction. *Conflict of Interest*: The authors have declared that no conflict of interest exists.

References

Araya R, Vogels TP, Yuste R. 2014. Activity-dependent dendritic spine neck changes are correlated with synaptic strength. Proc Natl Acad Sci USA. 111:E2895–E2904.

Awad PN, Sanon NT, Chattopadhyaya B, Carrico JN, Ouardouz M, Gagne J, Duss S, Wolf D, Desgent S, Cancedda L, et al. 2016. Reducing premature KCC2 expression rescues seizure susceptibility and spine morphology in atypical febrile seizures. Neurobiol Dis. 91:10–20.

Balakrishnan V, Becker M, Lohrke S, Nothwang HG, Guresir E, Friauf E. 2003. Expression and function of chloride transporters during development of inhibitory neurotransmission in the auditory brainstem. J Neurosci. 23:4134–4145.

Baldi R, Varga C, Tamas G. 2010. Differential distribution of KCC2 along the axo-somato-dendritic axis of hippocampal principal cells. Eur J Neurosci. 32:1319–1325.

Ben-Ari Y, Cherubini E, Corradetti R, Gaiarsa JL. 1989. Giant synaptic potentials in immature rat CA3 hippocampal neurones. J Physiol. 416:303–325.

Blaesse P, Guillemin I, Schindler J, Schweizer M, Delpire E, Khiroug L, Friauf E, Nothwang HG. 2006. Oligomerization of KCC2 correlates with development of inhibitory neurotransmission. J Neurosci. 26:10407–10419.

Bosch M, Hayashi Y. 2012. Structural plasticity of dendritic spines. Curr Opin Neurobiol. 22:383–388.

Cancedda L, Fiumelli H, Chen K, Poo MM. 2007. Excitatory GABA action is essential for morphological maturation of cortical neurons in vivo. J Neurosci. 27:5224–5235.

Chamma I, Heubl M, Chevy Q, Renner M, Moutkine I, Eugène E, Poncer JC, Lévi S. 2013. Activity-dependent regulation of the K/Cl transporter KCC2 membrane diffusion, clustering, and function in hippocampal neurons. J Neurosci. 33:15488–15503.

Chattopadhyaya B, Di Cristo G, Higashiyama H, Knott GW, Kuhlman SJ, Welker E, Huang ZJ. 2004. Experience and activity-dependent maturation of perisomatic GABAergic innervation in primary visual cortex during a postnatal critical period. J Neurosci. 24:9598–9611.

Chevy Q, Heubl M, Goutierre M, Backer S, Moutkine I, Eugene E, Bloch-Gallego E, Levi S, Poncer JC. 2015. KCC2 gates activity-driven AMPA receptor traffic through cofilin phosphorylation. J Neurosci. 35:15772–15786.

Chudotvorova I, Ivanov A, Rama S, Hübner CA, Pellegrino C, Ben-Ari Y, Medina I. 2005. Early expression of KCC2 in rat hippocampal cultures augments expression of functional GABA synapses. J Physiol. 566:671–679.

Dal Maschio M, Ghezzi D, Bony G, Alabastri A, Deidda G, Brondi M, Sato SS, Zaccaria RP, Di Fabrizio E, Ratto GM, et al. 2012. High-performance and site-directed in utero electroporation by a triple-electrode probe. Nat Commun. 3:960.

Di Cristo G, Awad PN, Hamidi S, Avoli M. 2018. KCC2, epileptiform synchronization, and epileptic disorders. Prog Neurobiol. 162: 1–16.

Duebel J, Haverkamp S, Schleich W, Feng G, Augustine GJ, Kuner T, Euler T. 2006. Two-photon imaging reveals somatodendritic chloride gradient in retinal ON-type bipolar cells expressing the biosensor Clomeleon. Neuron. 49:81–94.

Ferrini F, De Koninck Y. 2013. Microglia control neuronal network excitability via BDNF signalling. Neural Plast. 2013: 429815.

Fiumelli H, Briner A, Puskarjov M, Blaesse P, Belem BJ, Dayer AG, Kaila K, Martin J-LL, Vutskits L. 2013. An ion transport-independent role for the cation-chloride cotransporter KCC2 in dendritic spinogenesis in vivo. Cereb Cortex. 23:378–388.

Fiumelli H, Cancedda L, Poo MM. 2005. Modulation of GABAergic transmission by activity via postsynaptic Ca2+-dependent regulation of KCC2 function. Neuron. 48:773–786.

Fiumelli H, Woodin MA. 2007. Role of activity-dependent regulation of neuronal chloride homeostasis in development. Curr Opin Neurobiol. 17:81–86.

Galanopoulou AS. 2008. Sexually dimorphic expression of KCC2 and GABA function. Epilepsy Res. 80:99–113.

Gauvain G, Chamma I, Chevy Q, Cabezas C, Irinopoulou T, Bodrug N, Carnaud M, Levi S, Poncer JC. 2011. The neuronal K-Cl cotransporter KCC2 influences postsynaptic AMPA receptor content and lateral diffusion in dendritic spines. Proc Natl Acad Sci USA. 108:15474–15479.

Hotulainen P, Llano O, Smirnov S, Tanhuanpää K, Faix J, Rivera C, Lappalainen P. 2009. Defining mechanisms of actin polymerization and depolymerization during dendritic spine morphogenesis. J Cell Biol. 185:323–339.

Huang ZJ, Kirkwood A, Pizzorusso T, Porciatti V, Morales B, Bear MF, Maffei L, Tonegawa S. 1999. BDNF regulates the maturation of inhibition and the critical period of plasticity in mouse visual cortex. Cell. 98:739–755.

Kaila K, Price TJ, Payne JA, Puskarjov M, Voipio J. 2014. Cation-chloride cotransporters in neuronal development, plasticity and disease. Nat Rev Neurosci. 15:637–654.

Kaila K, Ruusuvuori E, Seja P, Voipio J, Puskarjov M. 2014. GABA actions and ionic plasticity in epilepsy. Curr Opin Neurobiol. 26:34–41.

Kellner Y, Gödecke N, Dierkes T, Thieme N, Zagrebelsky M, Korte M. 2013. The BDNF effects on dendritic spines of mature hippocampal neurons depend on neuronal activity. Front Synaptic Neurosci. 6:5.

Khalilov I, Chazal G, Chudotvorova I, Pellegrino C, Corby S, Ferrand N, Gubkina O, Nardou R, Tyzio R, Yamamoto S, et al. 2011. Enhanced synaptic activity and epileptiform events in the embryonic KCC2 deficient hippocampus. Front Cell Neurosci. 5:23.

Khirug S, Ahmad F, Puskarjov M, Afzalov R, Kaila K, Blaesse P. 2010. A single seizure episode leads to rapid functional activation of KCC2 in the neonatal rat hippocampus. J Neurosci. 30:12028–12035.

Korte M, Griesbeck O, Gravel C, Carroll P, Staiger V, Thoenen H, Bonhoeffer T. 1996. Virus-mediated gene transfer into hippocampal CA1 region restores long-term potentiation in brain-derived neurotrophic factor mutant mice. Proc Natl Acad Sci USA. 93:12547–12552.

Lee H, Chen CX, Liu Y-JJ, Aizenman E, Kandler K. 2005. KCC2 expression in immature rat cortical neurons is sufficient to switch the polarity of GABA responses. Eur J Neurosci. 21: 2593–2599.

Li H, Khirug S, Cai C, Ludwig A, Blaesse P, Kolikova J, Afzalov R, Coleman SK, Lauri S, Airaksinen MS, et al. 2007. KCC2 interacts with the dendritic cytoskeleton to promote spine development. Neuron. 56:1019–1033.

Llano O, Smirnov S, Soni S, Golubtsov A, Guillemin I, Hotulainen P, Medina I, Nothwang HG, Rivera C, Ludwig A. 2015. KCC2 regulates actin dynamics in dendritic spines via interaction with β-PIX. J Cell Biol. 209:671–686.

Ludwig A, Uvarov P, Soni S, Thomas-Crusells J, Airaksinen MS, Rivera C. 2011. Early growth response 4 mediates BDNF induction of potassium chloride cotransporter 2 transcription. J Neurosci. 31:644–649.

Mahadevan V, Dargaei Z, Ivakine EA, Hartmann AM, Ng D, Chevrier J, Ormond J, Nothwang HG, McInnes RR, Woodin MA. 2015. Neto2-null mice have impaired GABAergic

inhibition and are susceptible to seizures. Front Cell Neurosci. 9:368.

Markkanen M, Karhunen T, Llano O, Ludwig A, Rivera C, Uvarov P, Airaksinen MS. 2014. Distribution of neuronal KCC2a and KCC2b isoforms in mouse CNS. J Comp Neurol. 522: 1897–1914.

Merner ND, Chandler MR, Bourassa C, Liang B, Khanna AR, Dion P, Rouleau GA, Kahle KT. 2015. Regulatory domain or CpG site variation in SLC12A5, encoding the chloride transporter KCC2, in human autism and schizophrenia. Front Cell Neurosci. 9:386.

Mizuno K. 2013. Signaling mechanisms and functional roles of cofilin phosphorylation and dephosphorylation. Cell Signal. 25:457–469.

Nakayama AY, Harms MB, Luo L. 2000. Small GTPases Rac and Rho in the maintenance of dendritic spines and branches in hippocampal pyramidal neurons. J Neurosci. 20:5329–5338.

Niwa H, Yamamura K, Miyazaki J. 1991. Efficient selection for high-expression transfectants with a novel eukaryotic vector. Gene. 108:193–199.

Ouardouz M, Lema P, Awad PN, Di Cristo G, Carmant L. 2010. N-methyl-D-aspartate, hyperpolarization-activated cation current (Ih) and gamma-aminobutyric acid conductances govern the risk of epileptogenesis following febrile seizures in rat hippocampus. Eur J Neurosci. 31:1252–1260.

Patterson SL, Grover LM, Schwartzkroin PA, Bothwell M. 1992. Neurotrophin expression in rat hippocampal slices: a stimulus paradigm inducing LTP in CA1 evokes increases in BDNF and NT-3 mRNAs. Neuron. 9:1081–1088.

Pellegrino C, Gubkina O, Schaefer M, Becq H, Ludwig A, Mukhtarov M, Chudotvorova I, Corby S, Salyha Y, Salozhin S, et al. 2011. Knocking down of the KCC2 in rat hippocampal neurons increases intracellular chloride concentration and compromises neuronal survival. J Physiol. 589:2475–2496.

Puskarjov M, Ahmad F, Khirug S, Sivakumaran S, Kaila K, Blaesse P. 2015. BDNF is required for seizure-induced but not developmental up-regulation of KCC2 in the neonatal hippocampus. Neuropharmacology. 88:103–109.

Rinetti-Vargas G, Phamluong K, Ron D, Bender KJ. 2017. Periadolescent maturation of GABAergic hyperpolarization at the axon initial segment. Cell Rep. 20:21–29.

Rivera C, Li H, Thomas-Crusells J, Lahtinen H, Viitanen T, Nanobashvili A, Kokaia Z, Airaksinen MS, Voipio J, Kaila K, et al. 2002. BDNF-induced TrkB activation down-regulates the K^+–Cl^- cotransporter KCC2 and impairs neuronal Cl- extrusion. J Cell Biol. 159:747–752.

Rivera C, Voipio J, Thomas-Crusells J, Li H, Emri Z, Sipila S, Payne JA, Minichiello L, Saarma M, Kaila K. 2004. Mechanism of activity-dependent downregulation of the neuron-specific K-Cl cotransporter KCC2. J Neurosci. 24: 4683–4691.

Saneyoshi T, Wayman G, Fortin D, Davare M, Hoshi N, Nozaki N, Natsume T, Soderling TR. 2008. Activity-dependent synaptogenesis: regulation by a CaM-kinase kinase/CaM-kinase I/betaPIX signaling complex. Neuron. 57:94–107.

Shi Y, Pontrello CG, DeFea KA, Reichardt LF, Ethell IM. 2009. Focal adhesion kinase acts downstream of EphB receptors to maintain mature dendritic spines by regulating cofilin activity. J Neurosci. 29:8129–8142.

Tang X, Kim J, Zhou L, Wengert E, Zhang L, Wu Z, Carromeu C, Muotri AR, Marchetto MC, Gage FH, et al. 2016. KCC2 rescues functional deficits in human neurons derived from patients with Rett syndrome. Proc Natl Acad Sci U S A. 113:751–756.

Turrigiano GG, Leslie KR, Desai NS, Rutherford LC, Nelson SB. 1998. Activity-dependent scaling of quantal amplitude in neocortical neurons. Nature. 391:892–896.

Tyler WJ, Pozzo-Miller LD. 2001. BDNF enhances quantal neurotransmitter release and increases the number of docked vesicles at the active zones of hippocampal excitatory synapses. J Neurosci. 21:4249–4258.

Tyler WJ, Pozzo-Miller L. 2003. Miniature synaptic transmission and BDNF modulate dendritic spine growth and form in rat CA1 neurones. J Physiol. 553:497–509.

Zhang H, Webb DJ, Asmussen H, Horwitz AF. 2003. Synapse formation is regulated by the signaling adaptor GIT1. J Cell Biol. 161:131–142.